Optical constants detection in tin dioxide nano-size layers by surface plasmon resonance investigation

© B.K. Serdega, I.E. Matyash, L.S. Maximenko, S.P. Rudenko, V.A. Smyntyna*, V.S. Grinevich*¶, L.N. Filevskaya*, B. Ulug+, A. Ulug+, B.M. Yücel+

V.E. Lashkaryov Institute of Semiconductor Physics, National Academy of Sciences of Ukraine,
03028 Kiev, Ukraine
* Odessa National University named after I.I. Mechnikov,
65082 Odessa, Ukraine
+ Akdeniz University,
Antalya, Turkey

(Получена 13 апреля 2010 г. Принята к печати 2 июля 2010 г.)

Optical constants of tin dioxide nano-size layers were detected using surface plasmons resonance research technique. Squared reflectance indexes difference as well as the ones with *s*- and *p*-polarized light are measured simultaneously. Obtained in the work the refraction coefficient of the tin dioxide film gives the possibility to judge about the structural perfection of the layer and confirms that the film has significant porosity, which is created during the decomposition of the polymer materials used as structuring additives. It is shown that the resonance condition for surface plasmons may be destroyed through the interaction of surface plasmons with surface roughness potential of the film (medium dielectric properties variation).

1. Introduction

There is a constant tendency to use thin films as gas sensors due to the improved surface of nano-size materials [1,2]. One of such materials is tin dioxide which has perfect sensitivity to various gases and has superior chemical stability [3–5]. Tin dioxide films with nano-size grains can also be used as detectors for environmental monitoring [1,6,7]. Improvements in tin dioxide based nanowires and nanobelts are new structures and sensors for different chemicals [8–10].

A surface plasmon (SP) is an electromagnetic wave, excited by external radiation. This wave propagates at metal–dielectric interface and its electric field exponentially attenuates on opposite sides of the interface in both mediums along the normal to the surface. The waves' specific property is that their energy and attenuation are localized within an interface which makes them strongly dependent on the external medium dielectric parameters and structural perfection (composition uniformity, surface shape et. al.) of a metal. SP spectroscopic investigations of separate particles serve for refraction index detection of the medium (matrix) surrounding a particle. Such composition may be used as an optical nanosensor. Changes of such medium dielectric properties cause resonance frequency variations in the wide spectral range.

Surface plasmon resonance (SPR) occurs when electromagnetic waves are reflected off thin metal films. SPR is one of the most sensitive techniques actively developed to sense the changes in the dielectric function of a material. A fraction of electromagnetic energy incident at a well defined angle can interact with surface plasmons thus reducing the reflected light intensity. Since such plasmons are on the boundary of the metal–air/metal–liquid interfaces these oscillations are sensitive to any changes taking place on the metal surface, such as molecular adsorption and surface irregularities. Consequently, SPR is the basis of many tools for measuring adsorption onto metal surfaces and different lab-on-a-chip sensors.

For nanoparticles, localized surface plasmon oscillations exhibit strong absorption bands in the ultraviolet–visible regime whose exact energy depend on the relative position of the polarization of the light and the axis of symmetry of the nanowire [11]. Changes in the local index of refraction upon absorption to the nanoparticles shift the resonance. Such shift has found application in biochemistry [12] and in nanomaterials [13,14]. Use of polarized light for detecting SPR phenomenon in nanostructured oxides is now proved and is becoming an effective technique [15].

Polarization modulation of light is a known technique and incorporated to SPR in order to investigate pleochroism in photoconductivity [16], photovoltaic effects [17,18] and metal films [19]. Being a differential technique it gives reliable results even when the constituent signals lie below the noise level.

The present work is one of the first where polarization modulated spectroscopy of SPR is employed for the first time to a nanostructured tin dioxide film, which is known to be an *n*-type semiconductor containing enough charge carriers for formation of surface plasmons [20]. Results are used to discuss the film structure and the influence of surface morphology on resonance plasmon peaks.

2. Experiments

Experimental system used to measure the reflectivity is depicted in Fig. 1, whose details are given elsewhere [19]. Those will not be repeated here but summarized briefly. A nanostructured tin dioxide film is formed on a glass half cylinder in Kretschmann configuration as described in [16].

¶ E-mail: grinevich@onu.edu.ua

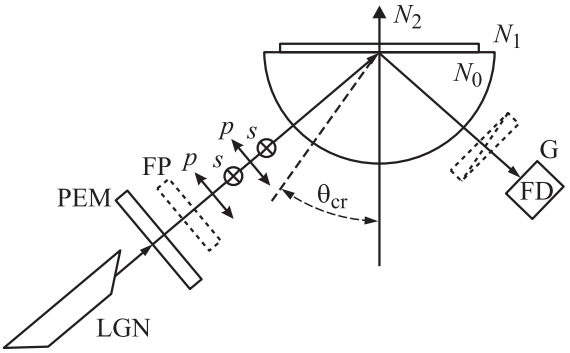

Fig. 1. Experimental setup. LGN — helium–neon laser, PEM — photoelastic polarization modulator, PF — phase plate; p, s — linear polatizators, azimuths are parallel and perpendicular to the plane of incidence; G — Glann prism, FD — photo detector, θ_{cr} — critical angle for the total internal reflection; N_0, N_1 and N_2 — refraction indices of glass, films and air, respectively.

In this technique, sample is successively illuminated by constant intensity s- and p-polarized light. Differential signal, which is the difference between the squared reflectance of s- (R_s^2) and p-polarization (R_p^2), $\Delta R = R_s^2 - R_p^2$, is then recorded. Using the system shown in Fig. 1 R_s^2, R_p^2 and ΔR are measured simultaneously. A 1/3 m monochromator associated with a halogen lamp is used as an unpolarized light source, which is replaced by a helium–neon laser whenever a linear polarized light at a fixed wavelength is required. Surface morphology of the film is investigated using an atomic force microscope (AFM) Nano Scope 111a in its tapping mode.

3. Results and discussion

Angular variations of R_s^2, R_p^2 and ΔR of the tin dioxide film are shown in Fig. 2, *a*. Reflectivity of s- and p-polarized light increases to a maximum at the critical angle (θ_{cr}) of total internal reflection around 44° and stays more or less constant for the angles higher than the angle of critical reflection. Above 65° they decrease sharply. However, ΔR reveals a steady increase until the angle of incidence reaches the vicinity of the critical angle of total internal reflection at which the sharp drop is monitored. At the critical angle of incidence above which the total internal reflection condition is broken, ΔR changes its sign. It should be noted that difference between R_s and R_p above the critical angle (see Fig. 2, *b*) indicates the strength of resonant interaction, which is reduced due to dispersion at potential relief caused by pores and surface roughness.

Using ultra thin gold films, it was shown [21] that the resonant character of the interaction of s- and p-polarized light with electrons influences the sign of ΔR at the angle of incidence higher than the critical angle. For the simultaneous resonant interaction of p- and s-polarized light with clusters ΔR will have positive values in this angular range.

In the present case negative sign is exclusively due to the resonance of p-polarized light. In fact, as seen from the Fig. 2, *b* the reflectance of p-polarized light first increases by 5.7% within 1° after the critical angle of incidence, then decreases by $\sim 2.5\%$ in the following 5° while the one of s-polarized light reveals steady increase of about 0.5% in 6° after the critical angle of incidence. This indicates the resonant nature of p-polarized light interaction with the film. Outside the resonance region, e. g. above 50° in Fig. 2, reflectance of s- and p-polarized light show steady increase in accord to each other up to 70°, above which both curves sharply drop.

Wavelength dependence of ΔR at the angle slightly above the critical angle of incidence, e. g. at 46°, depicted in Fig. 3 reveals that ΔR increases steadily as the wavelength increases. Refraction and absorption coefficients of the tin dioxide film, n and κ, respectively, are obtained after

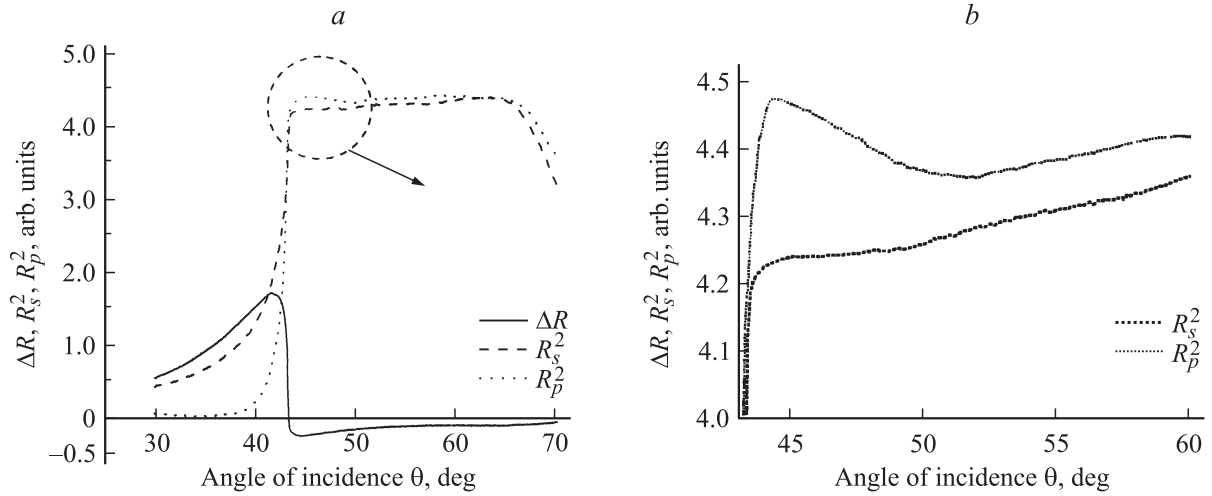

Fig. 2. Reflectance of s- and p-polarized light and differential reflectance vs. angle of incidence at 630 nm for the nanostructured tin dioxide film: *a* — total curves, *b* — R_s^2 and R_p^2 in the vicinity of the critical angle.

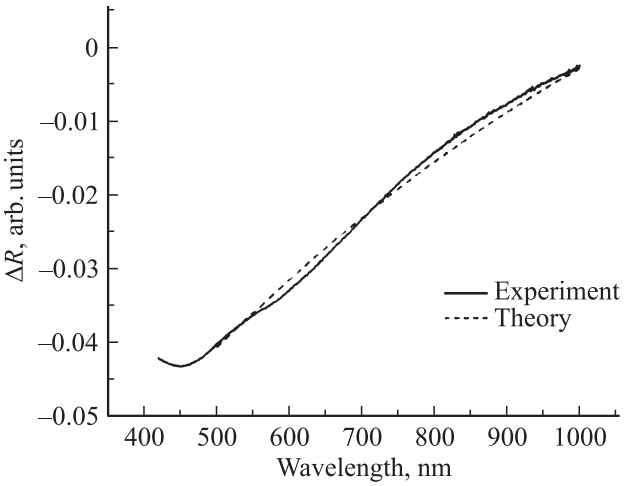

Fig. 3. Variation of differential reflectance with wavelength of incident light for the nanostructured tin dioxide film. The angle of incidence is fixed to 46°, slightly above the critical angle of incidence.

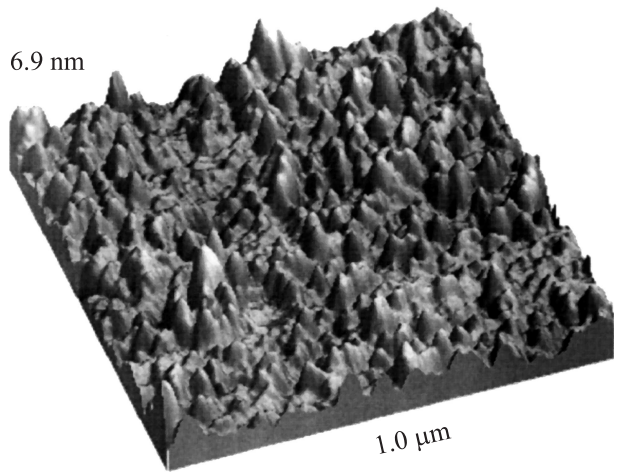

Fig. 4. AFM image of the film, which has roughness $\sim (5-10)$ nm in height and ~ 50 nm in width. Reliablity of lateral size is low due to convolution with the tip shape.

Fresnel equation [22] is fitted to experimental data by treating n and κ as adjustable parameters. Fitting is performed in the wavelength range $\lambda = 500-1000$ nm, $n = 1.28 + 0.000005\lambda$, $\kappa = 0.223-\lambda/4700$ were found within a confidence limit of $R^2 = 99.5$. Coefficients n and κ are both linearly dependent on wavelength. Refraction index obtained in this way at 632 nm for our tin dioxide sample, $n = 1.28315$, has a value between the value of bulk tin dioxide, 1.56, and the one of air, 1.003. This value of refraction index is consistent with the literature data [7] and suggests that the film has porous structure as it is expected due to the polymeric additives, which leaves a sponge-like structure after it decomposes during the annealing cycle [23].

The shape of the curve for $\theta > \theta_{cr}$ in Fig. 3 is primarily determined by the properties of incomplete internal reflection. It should be noted that ΔR vs. wavelength curve in Fig. 3 does not reveal a peak for $\theta > \theta_{cr}$ but displays negative ΔR values the same as the ultra thin gold film does [19]. Such a peak indicates the resonant interaction of light with surface plasmons and its intensity depends on film thickness in a nonlinear manner. For gold films, for example, it appears for the first time at 35 nm and reaches to a maximum value at the thickness of 50 nm and, then weakens before it fades away for the film thicker than ~ 250 mnm [15]. Film thickness is measured as ~ 10 nm (Fig. 4). Resonance peak for $\theta > \theta_{cr}$ should have been observed even for such a thin tin dioxide film since refration index estimated for the tin dioxide film at $\lambda = 632$ nm from Fig. 3, $n = 1.28315$, suggests that the effective thickness of tin dioxide is ~ 6 times greater that it is for gold with $n = 0.20$ [19], and, as being an n-type semiconductor, tin dioxide contains enough charge concentration for the formation of surface plasmons. However the result in Fig. 3 suggests that the resonance condition is not fully satisfied. This might be due to nanostructure as well as to surface roughness of the film since the surface plasmon wave propagating in the direction parallel to the film/air interface losts its energy every time it hits a local particle, surface roughness or grain boundaries. Such interactions of surface plasmons may destroy the resonance condition and thus, the resonant interaction of light with surface plasmons does not appear.

4. Conclusions

Surface plasmons resonance technique using modulated polarized light was applied to the nanostructured tin dioxide film and its refraction index as well as extinction coefficient are obtained. Refraction index of the film reveals that the tin dioxide film has a porous structure confirming the assessments for the existence of pores in the films.

It is argued that the resonance conditions for surface plasmons are destroyed by interaction of them with the surface roughness of the film (medium dielectric properties variation) and the squared reflectance indexes difference curve is primarily determined by total internal reflections. SPR technique employing semiconductor films with sufficiently high carrier density has potential to expand the application area of the technique.

The authors gratefully acknowledge the financial support of The Scientific and Technological Research Council of Turkey (TUBITAK) (grant N 107T277) and the support of Ministry of Ukraine for Education and Science (grant N M/349-2008). Authors gratefully acknowledge the considerable support of Lashkaryov Institute of Physics of Semiconductors, National Academy of Sciences of Ukraine. B. Ulug, A. Ulug and B.M. Yücel also acknowledge the support of Akdeniz University–Turkey.

References

[1] J. Homola, S.S. Yee, G. Gauglitz. Sensors Actuators B, **54**, 3 (1999).
[2] N. Yamazoe. Sensors Actuators B, **5**, 7 (1991).
[3] B. Hoffheins. *Handbook of Chemical and Biological Sensors*, ed. by R.F. Taylor, J.S. Schultz (Philadelphia, Institute of Physics, 1996).
[4] Y. Shimizu, M. Egashira. MRS Bulletin, **24**, 18 (1999).
[5] A. Kolmakov, M. Moskovits. Ann. Rev. Mater. Res., **34**, 151 (2004).
[6] M. Anastasescu, M. Gartner, S. Mihaiu, C. Anastasescu, M. Purica, E. Manea, M. Zaharescu. *Proc. Int. Semiconductor Conf.* (Sinaia, 2006) v. 1, p. 163.
[7] R. Rella, P. Siciliano, S. Capone, M. Epifani, L. Vasanelli, A. Liciulli. Sensors Actuators B, **58**, 283 (1999).
[8] M. Stadermann, S.J. Papadakis, M.R. Falvo, J. Novak, E. Show, Q. Fu, J. Liu, Y. Fridman, J.J. Boland, R. Superfine, S. Washburn. Phys. Rev. B, **69**, 201 402 (2004).
[9] M.T. Woodside, P.L. McEuen. Science, **296**, 1098 (2002).
[10] Y. Yaish, J.Y. Park, S. Rosenblatt, V. Sazonova, M. Brink, P.L. McEuen. Phys. Rev. Lett., **92**, 046 401 (2004).
[11] G. Weick, G.-L. Ingold, R.A. Jalabert, D. Weinmann. Phys. Rev. B, **74**, 165 421 (1996).
[12] L.K. Chau, Y.F. Lin, S.F. Cheng, T.J. Lin. Sensors Actuators B, **113**, 100 (2006).
[13] T.W. Ebbesen, H.J. Lezec, H.F. Ghaemi, T. Thio, P.A. Wolf. Nature, **391**, 667 (1998).
[14] A. Benabbas, V. Halte, J.Y. Bigot. Opt. Express, **13**, 8730 (2005).
[15] S.A. Hooker. *Proc.* „*Nanoparticles 2002*“ (N.Y., 2002) p. 1.
[16] I.E. Matyash, B.K. Serdega. Semiconductors, **38**, 657 (2004).
[17] V.G. Zykov, B.K. Serdega. Sov. Phys. Semicond., **25**, 1308 (1991).
[18] L.J. Berezhinsky, E.F. Venger, I.E. Matyash, A.V. Sachenko, B.K. Serdega. Semiconductors, **39**, 1122 (2005).
[19] L.J. Berezhinsky, L.S. Maksimenko, I.E. Matyash, S.P. Rudenko, B.K. Serdega. Opt. Spectrosc., **105**, 257 (2008).
[20] E. Comini, V. Guidi, C. Malagu, G. Martinelli, Z. Pan, G. Sberveglieri, Z.L. Wang. J. Phys. Chem. B, **108**, 1882 (2004).
[21] L.J. Berezhinsky, O.S. Litvin, L.S. Maksimenko, I.E. Matyash, S.P. Rudenko, B.K. Serdega. Opt. Spectrosc., **107** (2), 277 (2009).
[22] P. Lorrain, D.P. Corson, F. Lorrain. *Electromagnetic Fields and Waves*, 3rd edn. (W.H. Freeman and Co., N.Y., 1988).
[23] L.N. Filevskaya, V.A. Smyntyna, V.S. Grinevich. Photoelectronics. Inter-Universities scientific articles (Odessa), **15**, 11 (2006).

Редактор Л.В. Шаронова